Stimulated release of fluorescently labeled IgE fragments that efficiently accumulate in secretory granules after endocytosis in RBL-2H3 mast cells

Keli Xu[1,‡], Rebecca M. Williams[2], David Holowka[1,*] and Barbara Baird[1,*]

[1]Department of Chemistry and [2]Department of Applied and Engineering Physics, Cornell University, Ithaca, NY, USA
*Authors for correspondence at Department of Chemistry, Baker Laboratory, Cornell University, Ithaca, NY 14853-1301, USA (E-mail: bab13@cornell.edu)
‡Present address: Molecular and Cellular Physiology, Beckman Center, Stanford University School of Medicine, Stanford, CA 94305, USA

SUMMARY

Sensitization of RBL-2H3 mast cells with monomeric fluorescein-5-isothiocyanate (FITC)-labeled immunoglobulin E (IgE) results in slow but highly efficient accumulation of labeled IgE fragments in a pool of acidic peripheral vesicles that are visible by fluorescence microscopy after raising endosomal pH with ammonium chloride. Stimulation of cells containing these FITC-IgE fragments by aggregation of high affinity receptors for IgE (FcεRI) or by Ca^{2+} ionophore and phorbol 12-myristate 13-acetate results in release of FITC fluorescence from the cells, which can be monitored continuously with a spectrofluorometer. The fluorescence release process corresponds to cellular degranulation: it is prevented under conditions that prevent stimulated β-hexosaminidase release, and these two processes exhibit the same antigen dose-dependence and kinetics. Pulse-chase labeling reveals that aggregation of FITC-IgE bound to FcεRI at the cell surface causes internalization and delivery to the regulated secretory vesicles with a high efficiency similar to monomeric IgE-FcεRI, but more rapidly. Binding of Cy3-modified IgE to FcεRI results in labeling of the same secretory vesicles as in FITC-IgE-sensitized cells, and these Cy3-labeled vesicles can be observed by fluorescence microscopy without neutralization of intracellular compartments. Simultaneous three-photon microscopy of serotonin fluorescence and two-photon microscopy of Cy3 fluorescence reveals that these Cy3-labeled vesicles coincide with serotonin-labeled secretory granules. After stimulation of the cells via aggregation of IgE-FcεRI or addition of Ca^{2+} ionophore and phorbol 12-myristate 13-acetate, depletion of the Cy3 label from the intracellular vesicles is observed with confocal microscopy. These results provide strong evidence for the lysosomal nature of secretory granules in these cells. In addition, they provide the basis for a direct, real-time method for monitoring single cell degranulation.

Key words: Mast cells, Immunoglobulin E, Fc receptors, Regulated exocytosis

INTRODUCTION

For RBL-2H3 cells, a highly studied rat mast cell line, aggregation of FcεRI causes cellular degranulation and consequent release of preformed mediators, including histamine (Barsumian et al., 1981), serotonin (Taurog et al., 1979) and β-hexosaminidase (Ortega and Pecht, 1988). These cells are of mucosal mast cell lineage, based on morphological and histochemical criteria (Seldin et al., 1985). They lack the typical appearance of serosal mast cells from the rat peritoneum, which contain a large number of tightly packed dense granules in their cytoplasm that undergo explosive compound exocytosis after stimulation (Galli et al., 1984). However, exocytic granules in RBL-2H3 and peritoneal mast cells share an antigenic marker, an 80 kDa transmembrane protein, which is also found in lysosomes and lytic granules of natural killer cells but is absent from the exocytic granules of endocrine pituitary cells and exocrine pancreatic acinar cells (Bonifacino et al., 1986, 1989). This and other evidence suggests that secretory granules in natural killer cells, mast cells and other hematopoietic cells are actually regulated secretory lysosomes (Griffiths, 1996). A previously untested prediction of this hypothesis is that proteins internalized via the endocytic machinery and destined for degradation should be delivered to these secretory granules and released upon appropriate stimulation.

Little is known about the molecular events involved in the terminal steps of FcεRI-mediated exocytosis, although evidence exists for the involvement of GTP binding proteins (Gomperts, 1990). RBL-2H3 cells have a number of attractive features for studying regulated exocytosis, but a limitation of these cells has been the inability to routinely monitor receptor-mediated exocytosis of individual cells. Previous studies showed that monomeric immunoglobulin E (IgE) binds tightly to FcεRI on RBL-2H3 cells yielding a complex with a very long lifetime at the cell surface (Kulczycki et al., 1974; Isersky et al., 1979). Aggregation of this complex by multivalent antigen at 37°C causes rapid IgE-FcεRI endocytosis, such that 50-60% of these complexes are internalized with a half-time of approx. 5 minutes (Furuichi et al., 1984). This process,

which occurs via coated pits (Pfeiffer et al., 1985; Mao et al., 1993), delivers the aggregated IgE-FcεRI complexes to endosomal vesicles and lysosomes, where they undergo proteolytic degradation (Isersky et al., 1983). Unlike aggregation-dependent FcεRI-mediated-degranulation, this FcεRI endocytosis does not depend on extracellular Ca^{2+} (Furuichi et al., 1984) and is inhibited by cytochalasin D, an inhibitor of microfilament polymerization (Ra et al., 1989).

We previously characterized the quenching of fluorescein-5-isothiocyanate (FITC) fluorescence that occurs when FITC-IgE binds 2,4-dinitrophenyl (DNP)[1] ligands (Erickson et al., 1986; Holowka and Baird, 1996). In the course of studying the binding of multivalent 2,4-dinitrophenyl (DNP)-BSA to FITC-anti-DNP-IgE on RBL-2H3 cells under stimulating conditions (Xu et al., 1998), we were surprised to observe a time-dependent increase in FITC fluorescence that followed an initial quenching phase. Investigation of the basis for these observations revealed that internalized FITC-IgE is efficiently delivered to secretory vesicles that undergo exocytosis after cellular activation. These studies have led to simple fluorescence methods for directly monitoring the kinetics of stimulated exocytosis and for observing stimulated degranulation in individual cells. They also provide new support for a direct relationship between lysosomes in the endocytic pathway and regulated secretory granules in these cells.

MATERIALS AND METHODS

Reagents

FITC was purchased from Molecular Probes, Inc. (Eugene, OR). The amino-reactive carbocyanine probe, Cy3, was purchased from Biological Detection Systems, Inc. (Pittsburgh, PA). Cytochalasin D, 5-hydroxytryptamine (serotonin), phorbol 12-myristate 13-acetate (PMA) and the Ca^+ ionophore A23187 were purchased from Sigma Chemical Co. (St Louis, MO). Affinity-purified rabbit anti-fluorescein antibody was purchased from East Acre Biologicals (Southbridge, MA). Mouse monoclonal anti-DNP-IgE was purified from ascites cells (Liu et al., 1980) by affinity chromatography (Holowka and Metzger, 1982) and gel-filtration chromatography (Subramanian et al., 1996). Mouse monoclonal IgE specific for 5-(dimethylamino)-naphthalene-1-sulfonyl (DNS) was purified from the supernatant of a switch-variant hybridoma cell line 27-74 (Dangl et al., 1988) by affinity chromatography (Weetall et al., 1990). FITC-anti-DNP-IgE was prepared as previously described (Erickson et al., 1986) and, for some experiments, it was chromatographed on a Sepharose 12 HPLC gel permeation column (Pharmacia Fine Chemicals, Piscataway, NJ) to remove trace amounts of IgE aggregates. Cy3-anti-DNP-IgE was prepared according to the recommendation of the Cy3 manufacturer. Protein A-containing heat-killed *Staphylococcus aureus* was obtained from Calbiochem-Novabiochem Co. (San Diego, CA). The monovalent DNP ligand [ε-[(2,4-dinitrophenyl)amino]-caproyl]-L-tyrosine (DCT) was purchased from Biosearch, Inc. (San Rafael, CA). BSA, conjugated with an average of 15 DNP groups (DNP-BSA) or with an average of 14 DNS groups (DNS-BSA) were prepared as previously described (Weetall et al., 1993).

Cell preparation

RBL-2H3 cells (Barsumian et al., 1981) were grown in stationary culture (Taurog et al., 1979). For some experiments, cells were sensitized overnight with a 3- to 5-fold excess over FcεRI of Cy3-anti-DNP-IgE or FITC-anti-DNP-IgE or a mixture of 80% of FITC-anti-DNP-IgE and 20% of unlabeled-anti-DNS-IgE, such that the cell-surface FcεRI were saturated with these various IgE. After adherent cells were harvested with 1.5 mM EDTA in buffered saline (135 mM NaCl, 5 mM KCl, 20 mM Hepes, pH 7.4), they were washed by centrifugation for 8 minutes at 200 *g*, then resuspended in buffered saline solution (BSS: 135 mM NaCl, 5 mM KCl, 20 mM Hepes, 1.8 mM $CaCl_2$, 1 mM $MgCl_2$, 1.8 mM glucose, 0.1% gelatin, pH 7.4). In some experiments, cells were sensitized with labeled IgE after harvesting, washing and resuspension. In this case, cells at the density of approx. 1×10^7 cells/ml were mixed with a 3- to 5-fold excess of FITC-anti-DNP-IgE over FcεRI and rotated at 37°C for 60-75 minutes, then washed three times and resuspended in BSS.

Degranulation and spectrofluorometric measurements

RBL-2H3 cells in suspension ($1-2\times10^6$/ml) sensitized with appropriate IgE were stimulated with DNP-BSA or DNS-BSA, or with A23187 together with PMA, as indicated in the figure legends. In some experiments, 2 μM cytochalasin D was added prior to the stimulating reagents. Steady-state fluorescence measurements were made with an SLM 8000 fluorescence spectrofluorometer operated in ratio mode. FITC was excited at 490 nm and emission was monitored at 520 nm. For each experiment, 2.2 ml of FITC-IgE-labeled cells were placed in a 10×10×40 mm acrylic cuvette and stirred continuously in a thermostatic sample chamber. In these experiments, background fluorescence due to cells and buffers was less than 10% of the total signal.

For simultaneous measurements of stimulated degranulation and FITC fluorescence changes, 50 μl samples of the cells were removed from the cuvette at various times and put on ice immediately to stop degranulation. After centrifugation at 14,000 *g* for 2 minutes at 4°C, 25 μl samples were evaluated for β-hexosaminidase activity, released as previously described (Schwartz et al., 1981; Pierini et al., 1996).

Pulse-chase experiments

For pulse-chase experiments designed to measure the time course of FITC-IgE internalization and delivery to secretory granules, RBL-2H3 cells were washed by centrifugation, then resuspended in growth medium at 1.5×10^7 cells/ml. After addition of fivefold excess of FITC-anti-DNP-IgE over FcεRI at time (t)=0, the cells were rotated for 1 hour at 37°C to allow binding to reach steady state, then cells were washed twice and resuspended at 2×10^6 cells/ml. For the initial time points, a sample of cells was removed, and the remaining cells were separated into two equal volumes. 1.6 μg/ml anti-IgE was added to one of these samples at t=1.5 hours, and both samples were continuously rotated at 37°C.

The initial time point sample of cells was centrifuged and resuspended in BSS at 2×10^6 cells/ml for degranulation and spectrofluorometric measurements. 2 ml samples of these cells were transferred to two cuvettes and maintained at 37°C, and 2 μM cytochalasin D, 50 nM PMA and 100 nM A23187 were added sequentially to one cuvette to stimulate maximal degranulation and the accompanying enhancement of FITC fluorescence. 1.6 μg/ml anti-IgE was added to the second cuvette to aggregate FcεRI and induce internalization of receptor aggregates. Under these conditions, internalization detected as FITC quenching reached a steady state after 1.5 hours, and these cells were then stimulated with cytochalasin D, PMA and A23187. 50 μl samples of cells were removed before and after stimulation to measure β-hexosaminidase release, as described above. For this and later time points, approx. 20% of the cellular β-hexosaminidase was released due to anti-IgE crosslinking of FcεRI prior to stimulation by PMA and A23187 in the presence of cytochalasin D. Greater than 70% of residual β-hexosaminidase was released due to this latter stimulation (data not shown). For later time points, samples of cells were removed from each of the two rotating samples (± anti-IgE), washed, and resuspended in BSS at 2×0^6 cells/ml for degranulation and spectrofluorometric measurements, as described for the initial time point.

The FITC fluorescence released after stimulation, $F_{releasable}$, was

calculated by subtracting the initial cell-associated fluorescence ($F_{initial}$) from the fluorescence after the stimulated fluorescence increase ($F_{stimulated}$) reached a steady state:

$$F_{releasable} = F_{stimulated} - F_{initial} \qquad (1)$$

0.025% Triton X-100 was added at the end of each stimulation measurement to permeabilize the cells and thereby determine the total cell-associated fluorescence (F_{total}). The quenched internal FITC fluorescence, $F_{internal}$, is calculated as:

$$F_{internal} = F_{total} - F_{initial} . \qquad (2)$$

Immunoprecipitation and SDS-PAGE analysis

5 ml of $2{\times}10^7$ RBL-2H3 cells/ml that had been sensitized with FITC-IgE overnight were suspended in BSS and stimulated with 500 ng/ml DNP-BSA in the presence of 3 μM cytochalasin D for 1 hour at 37°C. The cells were maintained in suspension by continual rotation, and an identical cell sample with 3 μM cytochalasin D in the absence of antigen was rotated in parallel as a control. The cells were sedimented by centrifuging for 10 minutes at 200 g, and the supernatants were then centrifuged at 14,000 g for 2 minutes at 4°C to remove any remaining particulate material. DCT (18 μM) was added to each sample to dissociate any DNP-BSA that might be bound to the FITC-labeled IgE/IgE fragments in the supernatants. Rabbit anti-fluorescein antibody (9 μg/ml) was added to each sample, and these were rotated at 4°C for 1 hour. 225 μl of prewashed, heat-killed *S. aureus* (containing protein A) was then added and rotation was continued at 4°C for 1 hour. The *S. aureus*-bound immunoprecipitates were washed once by centrifugation and resuspension in cold BSS and then boiled in 300 μl 2× sample buffer [0.1 M Tris-HCl, 20% glycerol, 2% SDS (w/v), pH 6.8]. The supernatant was then concentrated and analyzed by 10% SDS-PAGE under reducing conditions. The gel was illuminated in a 302 nm wavelength UV transilluminator immediately after electrophoresis, and fluorescence photographs were taken with a Polaroid MP-4 Land camera with a 520 nm filter and Polaroid MP-4 Land camera instant film.

Confocal and multiphoton fluorescence microscopy

Fluorescently labeled cells ($1{\times}10^7$/ml) were imaged with a BioRad MRC 600 confocal apparatus (BioRad, Cambridge, MA) in conjunction with a Zeiss Axiovert 10 microscope. The 568 nm line of a krypton-argon ion laser was selected for excitation of Cy3, and 585 nm dichroic and 585 nm long pass filters were used to monitor Cy3 emission. The 488 nm line of the krypton-argon ion laser was selected for excitation of fluorescein, and 510 nm dichroic and 515 nm long pass filters were used to monitor fluorescein emission. Chromatically corrected 100× or 63× objectives (N.A. 1.4) were employed. Confocal fluorescence images collected with the BioRad Comos software were analyzed with Adobe Photoshop image analysis software (Adobe Systems, Inc., San Jose, CA). In some experiments, differential interference contrast images were collected simultaneously with the fluorescence confocal images.

For FITC-IgE-labeled RBL-2H3 cells, 15 mM NH_4Cl was added to some samples to raise the pH of the acidified intracellular compartments (Ohkuma and Poole, 1978). For stimulation of Cy3-IgE-labeled RBL-2H3 cells, 500 μl of $1{\times}10^7$ cells/ml were stirred continuously at 37°C, and antigen or A23187 and PMA were added. Samples of cells were taken at various times and placed between glass slides and No. 1 coverslips for confocal imaging.

For the multiphoton imaging experiments, cells were plated onto 35 mm coverslip-bottomed dishes (Matek Corp., Ashwell, MA), cultured overnight in the presence of 1.5 μg/ml Cy3-IgE and 0.10 mM serotonin, washed twice and imaged in BSS. The microscopy apparatus used was similar to that described previously by Maiti et al. (1997). The illumination source was provided by an 80 MHz modelocked, 740 nm beam from an argon-pumped Ti:Sapphire laser (Tsunami, Spectra Physics, Mountain View, CA). Pulse widths,

measured with a Femtochrome XR-100 autocorrelator, were typically 70-80 fseconds. The characterized beam was directed in a double pass through two SF-10 prisms (CVI Laser Corp., Albuquerque, NM) to pre-chirp the pulses in compensation for dispersion effected principally by the microscope objective, a Zeiss 40×/1.3 NA F Fluar. After the prisms, the beam was attenuated and directed into a retrofitted BioRad MRC-600 confocal scanning box interfaced with a Zeiss Axiovert-35 microscope.

Because multiphoton excitation is intrinsically localized, confocal detection optics are unnecessary. To avoid signal degradation by extraneous optical elements, the fluorescence was separated from the excitation light by a 670 nm, long-pass dichroic mirror (all optical filters are from Chroma Technology Corp., Brattleboro, VT) placed between the microscope and the confocal scanner box. The fluorescence is further separated into Cy3 and serotonin channels using a 400 nm long-pass dichroic. The fluorescence in the serotonin channel (320-380 nm) was spectrally filtered with a 2 cm thick, 1 M $CuSO_4$ solution and a 2 mm thick piece of UG11 glass, and the fluorescence in the Cy3 channel (500-650 nm) was filtered with a wide-band emission filter (575DF150). The resulting fluorescence signals were detected with bialkali and multialkali photomultiplier tubes, respectively (HC125-02 and HC125-01, Hamamatsu Corp., Bridgewater, NJ), and transmitted through the external junction box to the MRC-600 integrators. The standard BioRad confocal microscopy software was used to acquire, view and analyze images.

Because the Cy3 is excited by a two-photon process and the serotonin is excited by a three-photon process, their image intensities depend to different extents on the illumination intensity. This fact is used to achieve optimal dual-signal imaging with no bleed-through between channels. The image pairs are acquired sequentially (Cy3, then serotonin, 3 seconds apart) with a tenfold higher illumination for the serotonin imaging (12 mW at the specimen). Control images from (1) cells that were Cy3-labeled but unloaded with serotonin and (2) cells that were serotonin-loaded but unlabeled with Cy3, revealed no fluorescence from the serotonin in the Cy3 channel and no fluorescence from the Cy3 in the serotonin channel.

The co-localization image analysis is accomplished by first measuring reference intensity values. For each of the two channels the background mean intensity values within the cells (μ) and their standard deviations (σ) were determined by averaging ten cytoplasmic regions within cells that (by eye) have no granules. Pixel distributions throughout the image stack are analyzed by defining *granule pixels* as those possessing values greater than μ+3σ. Analysis was carried out on 39 pairs of smoothed images (5×5 Gaussian kernel) representing more than 600 cells in all. For each image pair the co-localization fraction is defined as N_{CS}/N_C, where N_{CS} is the number of pixels that fit the granule criteria in both the Cy3 and serotonin images and N_C is the number of pixels that fit the granule criteria in the Cy3 image. To control for coincidental co-localization, the same analysis is performed on randomized pairs of images.

RESULTS

We used an established fluorescence quenching method (Erickson et al., 1986) to monitor binding of multivalent DNP-BSA to FITC-anti-DNP-IgE-FcεRI on the surface of RBL-2H3 cells. Fig. 1a shows the time course for binding of 2 μg/ml DNP-BSA to suspended cells ($2{\times}10^6$ cells/ml) at 35°C. In these experiments, cytochalasin D (2 μM) was added just prior to antigen to prevent aggregation-dependent internalization of FITC-IgE-FcεRI complexes, a process that causes additional quenching of FITC fluorescence due to the low endosomal pH environment experienced by internalized complexes (data not shown). Cells in Fig. 1a were sensitized with excess FITC-IgE
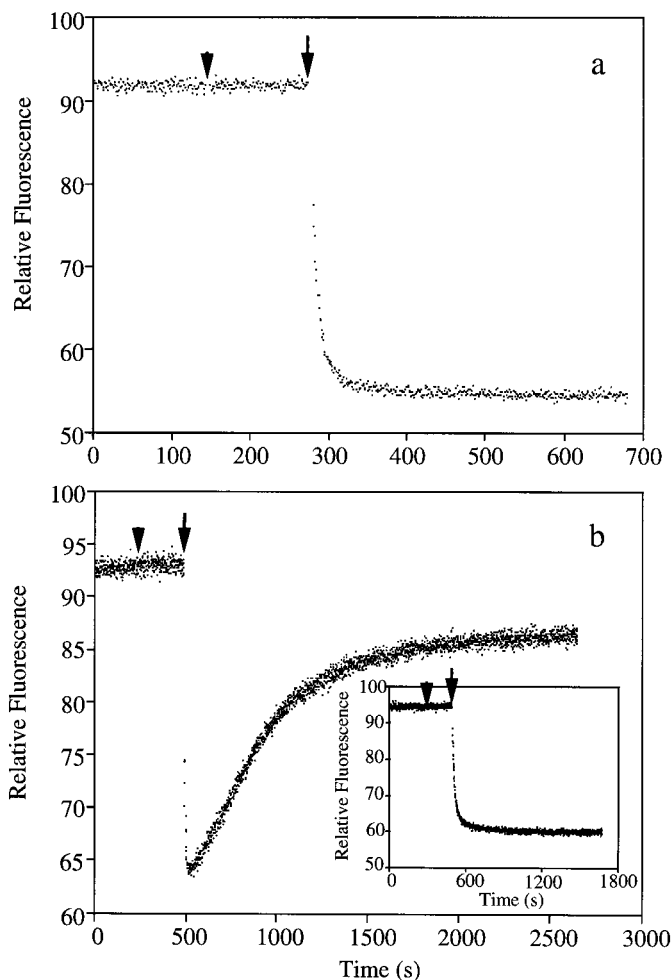
Fig. 1. Changes in fluorescence of FITC-anti-DNP-IgE bound to RBL-2H3 cells after addition of DNP-BSA. Cells were sensitized with excess FITC-IgE for 1 hour (a) or overnight (b). Washed, suspended cells were maintained at 35°C while 2 μM cytochalasin D was added to cells (arrowheads) followed by addition of 2 μg/ml DNP-BSA (arrows). Inset to (b) shows overnight-sensitized cells that were then maintained at 15°C during treatment with cytochalasin D and antigen.

Fig. 2. Stimulation of FITC fluorescence enhancement correlates with the stimulation of cellular degranulation. RBL-2H3 cells were sensitized overnight with a mixture of 80% FITC-anti-DNP-IgE and 20% unlabeled anti-DNS-IgE and washed. Suspended cells were maintained at 35°C and treated with 2 μM cytochalasin D just before addition of DNS-BSA (arrows) at a concentration of 50 ng/ml (a) or 5 ng/ml (b). In a, cells represented by the lower trace were pre-treated overnight with 75 nM PMA to prevent stimulated degranulation, and in b cells represented by the lower trace were stimulated in BSS lacking Ca^{2+}. The lower curves are offset from the upper curves to allow direct comparison.

for 1 hour at 37°C prior to washing and resuspension for the binding experiment. At the dose of antigen used, degranulation is maximal (data not shown) and binding occurs rapidly, nearing a steady state value after approx. 100 seconds. Cells in Fig. 1b were sensitized overnight at 37°C with a similar excess of FITC-IgE. For the cells sensitized overnight, the rapid phase of FITC quenching due to DNP-BSA binding is followed by a slower increase in FITC fluorescence that reaches a steady state with a half-time of approx. 400 seconds. As shown in Fig. 1b (inset), binding of DNP-BSA to these same cells at 15°C occurs with fluorescence quenching but without the subsequent fluorescence increase.

The relationship of stimulated increase in FITC fluorescence to stimulated degranulation.

The results in Fig. 1 and a series of related experiments suggested that the increase in FITC fluorescence observed for overnight-sensitized cells at 35°C (but not at 15°C) is due to
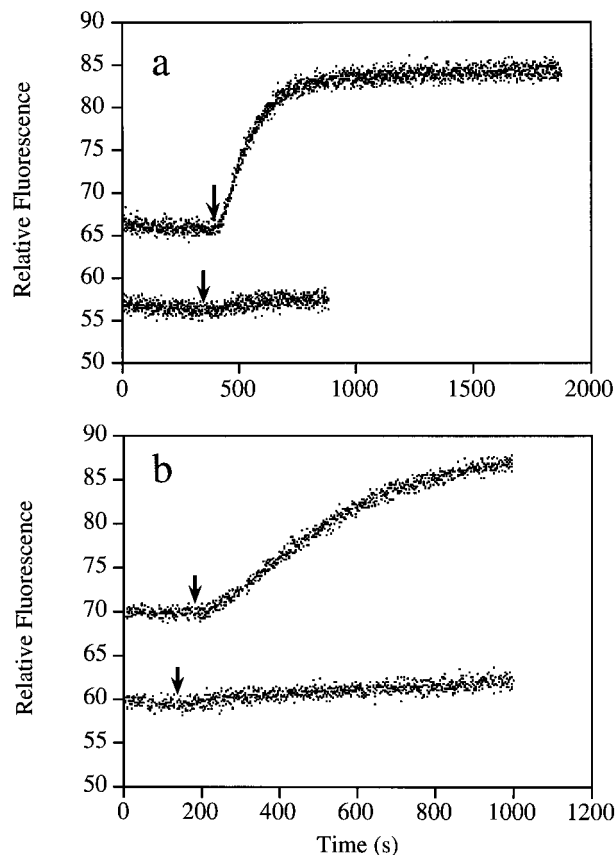
activation of later events in cell stimulation. Multivalent antigen stimulates the initial activation steps of the tyrosine kinase cascade at temperatures as low as 4°C (Field et al., 1997), but it does not stimulate more downstream events, such as inositol phosphate production, Ca^{2+} mobilization, and degranulation below about 20°C (WoldeMussie et al., 1986). To investigate this process more selectively, we altered our experimental conditions to eliminate the initial quenching of FITC fluorescence due to antigen binding (as seen in Fig. 1). By sensitizing the cells overnight with a mixture of 80% FITC-anti-DNP-IgE and 20% unlabeled anti-DNS-IgE, the cells can be fluorescently labeled as in Fig. 1, but triggered with a multivalent antigen (DNS-BSA) that does not bind to FITC-anti-DNP-IgE and does not cause FITC fluorescence quenching.

As seen in the upper traces in Fig. 2a,b, a time-dependent FITC fluorescence increase is triggered by DNS-BSA in the presence of cytochalasin D at 35°C. This response is significantly slower in Fig. 2b because a lower dose of antigen
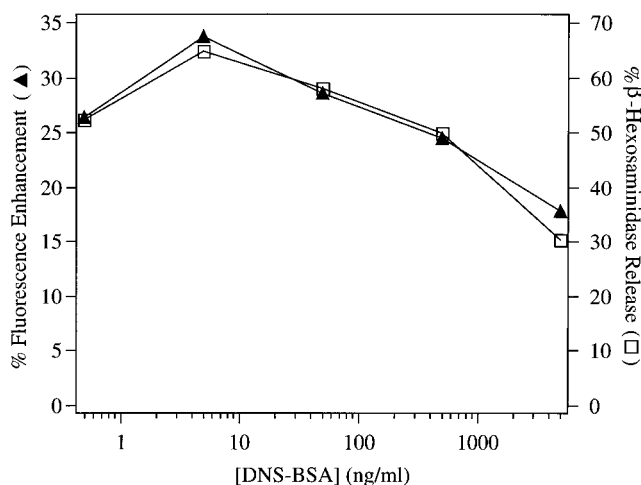
Fig. 3. Dose-dependence of FITC fluorescence enhancement (▲) and β-hexosaminidase release (□). RBL-2H3 cells were sensitized overnight with a mixture of 80% FITC-anti-DNP-IgE and 20% unlabeled anti-DNS-IgE. Cells were pretreated with 2 μM cytochalasin D, and FITC fluorescence enhancement was monitored after addition of DNS-BSA at 35°C. % Fluorescence enhancement represents the percentage increase in FITC fluorescence over the unstimulated fluorescence intensity after the stimulated increase reached a constant value. % β-hexosaminidase represents the percentage of total cellular β-hexosaminidase activity released when the fluorescence enhancement reached a plateau.

Fig. 4. Kinetics of stimulated FITC fluorescence enhancement (dots) compared to stimulated β-hexosaminidase release in the presence (△, upper curves) and absence (○, lower curves) of cytochalasin D. (a) Cells sensitized as in Figs 2 and 3 were stimulated with 5 ng/ml DNS-BSA (arrow for upper curve, arrowhead for lower curve) at 37°C. (b) Cells sensitized overnight with FITC-anti-DNP-IgE were stimulated with 50 nM PMA and 100 nM A23187 (arrow for upper curve, arrowhead for lower curve) at 35°C.

was used than in Fig. 2a, under conditions in which the rate of receptor crosslinking limits the rate of signaling (Xu et al., 1998). Conditions under which this fluorescence increase is prevented are also those under which degranulation is prevented: the lower trace in Fig. 2a shows that overnight treatment with 75 nM PMA prevents the fluorescence enhancement response at 35°C. These are conditions which also prevent stimulated serotonin release (Chang et al., 1995; White and Metzger, 1988), even though Ca^{2+} mobilization is not inhibited (Cunha-Melo et al., 1989; M. Weetall, D. Holowka and B. Baird, unpublished results). The lower trace in Fig. 2b shows that only a slow, small increase in FITC fluorescence occurs in the absence of extracellular Ca^{2+}. This also indicates a correlation between FITC fluorescence enhancement and stimulated exocytosis, as the latter process is strongly dependent on the influx of extracellular Ca^{2+} (Mohr and Fewtrell, 1987). As for stimulation by DNP-BSA in Fig. 1b, DNS-BSA does not cause FITC fluorescence enhancement at 15°C (data not shown).

Fig. 3 shows parallel antigen dose-response curves obtained for stimulation of the FITC fluorescence increase and for stimulation of β-hexosaminidase release, which is an established indicator of FcεRI-mediated exocytosis for these RBL-2H3 cells (Ortega and Pecht, 1988; Alber et al., 1992) and serosal mast cells (Schwartz et al., 1981).

Fig. 4a shows that the kinetics of antigen-stimulated FITC fluorescence enhancement and β-hexosaminidase release are identical, both in the presence and in the absence of cytochalasin D. As previously shown (Narasimhan et al., 1990; Seagrave and Oliver, 1990), pretreatment with cytochalasin D increases the rate of antigen-stimulated exocytosis, and
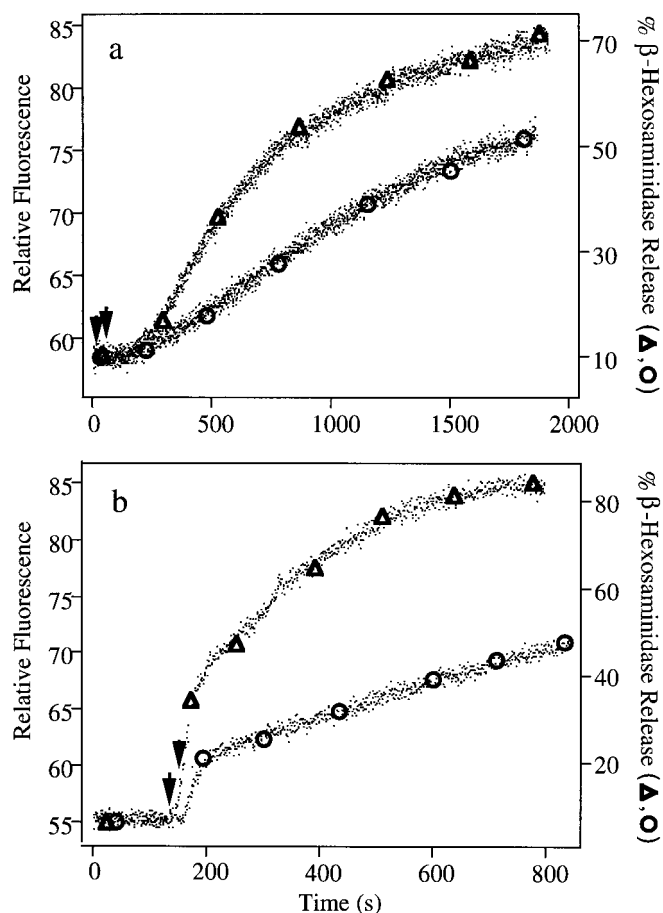
sometimes also increases the magnitude of the response. As shown in Fig. 4b, similar results are obtained when cells are stimulated by Ca^{2+} ionophore A23187 in the presence of PMA. In this case, surface IgE-FcεRI are not involved, yet cytochalasin D has a similar effect on both β-hexosaminidase and FITC fluorescence enhancement, and the kinetics of these two processes are identical. In the presence of cytochalasin D, more than 80% of the β-hexosaminidase is released in response to ionophore and PMA and more than 70% is released in response to antigen. It is notable that two distinct phases of exocytosis are detectable for the responses to ionophore and PMA, and this is best defined in the real-time response monitored continuously by the FITC fluorescence increase. We conclude from the results shown in Figs 1-4 that the stimulated increase in FITC fluorescence observed after overnight sensitization with FITC-IgE parallels the degranulation response in RBL-2H3 cells and provides a simple method for monitoring the kinetics of this process with adequate time resolution that is sufficient for detailed studies of the kinetics of stimulated exocytosis.

The stimulated increase in FITC-fluorescence is due to release of FITC-IgE fragments from acidic intracellular vesicles

When RBL-2H3 cells are sensitized overnight with excess FITC-IgE, washed and stimulated to undergo degranulation, FITC fluorescence is detected in the supernatant after centrifugation to remove the cells. In the absence of stimulation, a much smaller amount of FITC fluorescence is detected in the supernatant. The difference between the supernatant FITC fluorescence from stimulated and unstimulated cells is similar in magnitude to the FITC fluorescence enhancement observed when stimulated cells are monitored continuously in the fluorometer as in Figs 2 and 4 (data not shown). This suggests that the FITC fluorescence increase observed by steady state fluorometry is due to the release of cell-associated FITC from a state in which its fluorescence is highly quenched. As shown in Fig. 5, confocal images of FITC-IgE-sensitized cells are consistent with this explanation. In BSS, cells sensitized for either a short time (approx. 1 hour; Fig. 5a) or overnight (Fig. 5b) show mostly uniform surface fluorescence, with little or no intracellular fluorescence detectable in equatorial images. Fig. 5c shows that a similar result is obtained for short-term sensitized cells when they are exposed to 15 mM NH_4Cl to neutralize acidic intracellular vesicles (Ohkuma and Poole, 1978).

A very different result is obtained when NH_4Cl is added to cells sensitized overnight with FITC-IgE. As shown in the partial z-series of images from a single cell in Fig. 5d-h, a substantial amount of intracellular FITC fluorescence can be seen under these conditions in the form of discrete vesicles of various sizes and distributions throughout the cytoplasm. In these images, the kidney-shaped nucleus on the right side of the cell can be seen to exclude fluorescence in Fig. 5f-h, and

the brightest intracellular label is distributed near the periphery of the cell. Little or no FITC fluorescence is seen in the perinuclear region where the Golgi complex is expected near the middle of the nuclear cusp. This distribution of fluorescence is typical for most of the cells incubated overnight in this manner, and it contrasts markedly with the distribution of FITC-IgE observed shortly after undergoing antigen- or anti-IgE-mediated endocytosis. The latter intracellular FITC-IgE can be readily observed without NH_4Cl to neutralize the endosomes, appearing at earliest times in peripheral early endosomes and within minutes as bright spots in the perinuclear region near the center of the cell (Fig. 5i; Robertson et al., 1986).

The results shown in Fig. 5d-h indicate that a substantial amount of FITC-IgE associated with RBL-2H3 cells after overnight incubation is delivered to a population of peripheral intracellular vesicles. That this internal fluorescence is not detected in the absence of NH_4Cl indicates that the internalized FITC-IgE are localized to highly acidic vesicles. These results further suggest that the increase in FITC fluorescence detected after stimulation of the overnight-sensitized cells (Figs 1-4) is due to the release of this intracellular FITC to the external medium at neutral pH, where it fluoresces with a much higher quantum yield. After overnight sensitization, approx. 40% of the total cell-associated FITC-IgE is internal, as determined by comparing the FITC fluorescence before and after addition of Triton X-100 to lyse the cells (equation 2). The FITC fluorescence increase observed after maximal stimulation of overnight-sensitized cells with antigen or ionophore and PMA (Fig. 4; equation 1) is 25-30% of the total FITC observed after lysis with Triton X-100. This indicates that 63-75% of the intracellular FITC is released after stimulation.
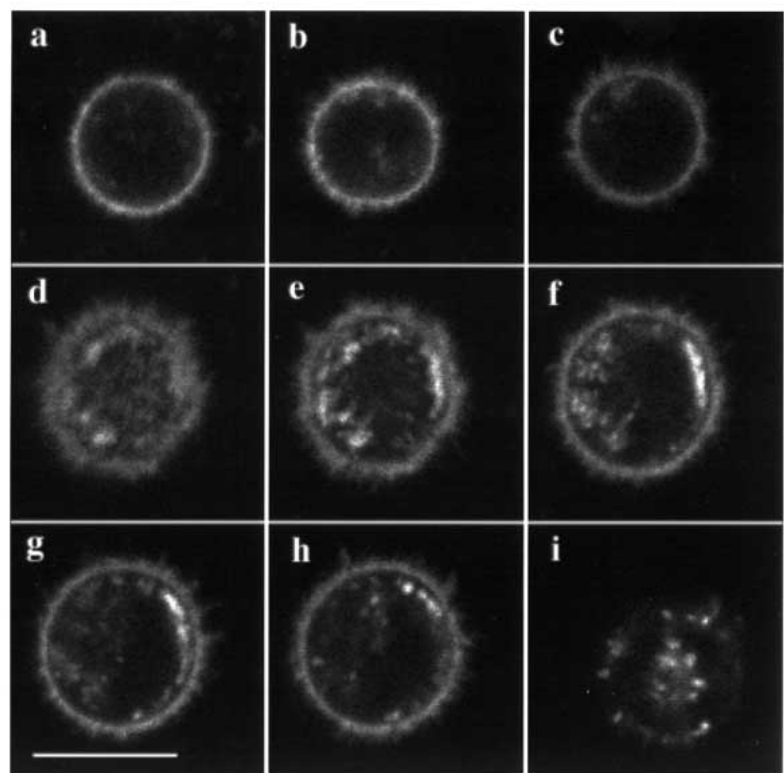
To examine the form of FITC-IgE released from the

Fig. 5. Confocal fluorescence images of cells sensitized with FITC-anti-DNP-IgE for 1 hour (a,c,i) or overnight (b,d-h). In c and d-h, 15 mM NH_4Cl was added to the cell samples to raise the pH of their acidified intracellular compartments prior to imaging. In i, the cell sample was incubated with 22 μg/ml rabbit anti-IgE antibody for approx. 15 minutes at 37°C to crosslink cell surface IgE-FcεRI and cause its internalization. a, b, c and i show the equatorial images of the cells. d-h show a partial z-series of images of a single cell. The thickness of each section is 0.7 μm. Bar, 10 μm.
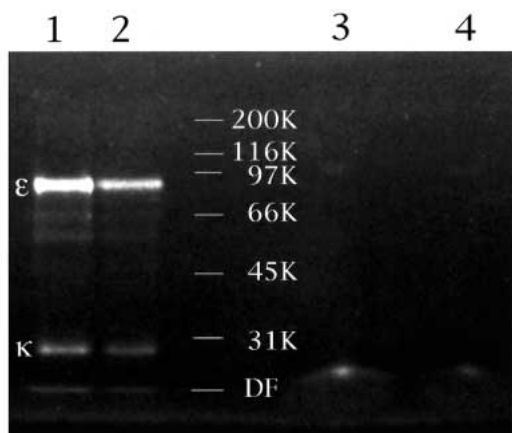
Fig. 6. Fluorescence image of FITC-labeled proteins that were released from RBL-2H3 cells sensitized with FITC-anti-DNP-IgE overnight and resolved by SDS-PAGE under reducing conditions. For comparison, lanes 1 and 2 contain 2 μg and 1 μg of stock FITC-IgE, respectively. The anti-fluorescein immunoprecipitate from the supernatant of antigen-stimulated (500 ng/ml DNP-BSA; lane 3) and unstimulated (lane 4) cells are shown. The apparent molecular masses of standard proteins are indicated, DF indicates the dye front, and ε and κ indicate the position of IgE heavy and light chains, respectively.

intracellular vesicle, 10^8 cells sensitized overnight with FITC-IgE and stimulated or not with an optimal dose of antigen were immunoprecipitated with rabbit anti-fluorescein antibody. Fig. 6 shows a fluorescence image of immunoprecipitated FITC analyzed by SDS-PAGE under reducing conditions. Lanes 3 and 4 show the fluorescence products immunoprecipitated from the supernatants of stimulated and unstimulated cells, respectively. A very faint fluorescent band is detected at a molecular mass that is slightly larger than the ε chain standards located in lanes 1 and 2, but most of the fluorescence present appears at or near the dye front. As expected, there is significantly more fluorescence near the front for the sample stimulated prior to immunoprecipitation of the supernatants. The location of this band is consistent with the stimulated release of FITC fragments of IgE that are less than about 25 kDa in size. From these results and two other similar experiments, we conclude that most of the FITC-IgE released upon stimulation is in the form of low molecular mass fragments, probably due to proteolytic digestion of FITC-IgE that is internalized during the overnight sensitization. Consistent with this explanation, we find that the intracellular FITC fluorescence seen in larger vesicles after treatment with NH₄Cl is uniformly distributed within the interior of these vesicles (Fig. 5 and data not shown) rather than located at their periphery, as expected for undigested IgE that would remain bound to membrane-associated receptors.

Accumulation in secretory vesicles is similarly efficient for aggregated and non-aggregated internalized FITC-IgE

Since previous studies on RBL-1 cells showed little evidence for internalization of monomeric IgE bound to FcεRI (Isersky et al., 1979), we examined carefully the overnight uptake of FITC-IgE and delivery to secretory granules in RBL-2H3 cells.

In one experiment, cells were incubated overnight with the same concentration of FITC-IgE used previously, but binding to FcεRI was blocked by the presence of a 20-fold excess of unlabeled IgE added prior to FITC-IgE. As expected, very little cell-associated FITC fluorescence was detected in the presence or absence of Triton X-100 (<10% of the control sample without unlabeled IgE). These results indicate that slow uptake of nanomolar concentrations of FITC-IgE into the low pH secretory vesicles occurs primarily via an FcεRI-specific pathway. To determine whether the uptake of FITC-IgE and delivery into secretory vesicles during overnight sensitization occurs with strictly monomeric IgE bound to FcεRI, we chromatographed FITC-IgE on a gel permeation column to separate monomeric FITC-IgE from a small amount of aggregates. Addition of this strictly monomeric FITC-IgE to unsensitized cells resulted in overnight labeling of the intracellular vesicles, similar to the results with unfractionated FITC-IgE. Also, similar release of intracellular FITC was observed after stimulation. In another experiment, a sample from the gel permeation monomer peak was re-chromatographed, and the resulting monomer FITC-IgE peak was used to sensitize cells overnight. Identical labeling of the low pH secretory vesicles was observed. Together, these results confirm that the secretory vesicles are labeled by an endocytic pathway that slowly internalizes monomeric IgE-FcεRI and then degrades the IgE to low molecular mass products that are retained in these compartments until exocytosis is stimulated.

The results described above, in conjunction with previous studies documenting the slow turnover of surface IgE-FcεRI (Furuichi et al., 1985; Quarto et al., 1985), indicate that the delivery of internalized FITC-IgE to the secretory granules is a highly efficient process. In order to investigate this more quantitatively, RBL-2H3 cells were pulse-labeled with saturating amounts of monomeric FITC-IgE for 1 hour at 37°C, followed by washing to remove unbound FITC-IgE and subsequent incubation for various times at 37°C to assess the time courses of internalization and delivery of FITC-IgE to secretory granules. To determine the effect of aggregation of FITC-IgE-FcεRI on these processes, a portion of the sensitized cells were treated with anti-IgE, and the amounts of unquenched surface FITC-IgE and low pH-quenched internalized FITC-IgE were assessed together with the amount of FITC-IgE released after stimulation with A23187 and PMA under optimal conditions.

Fig. 7 shows the results from one of two pulse-chase experiments which showed the same trends. In Fig. 7a, the time course of internalization of FITC-IgE bound to FcεRI as monitored by FITC quenching (equation 2) is compared for cells treated with anti-IgE (□; addition at arrow) or untreated (○). Consistent with the results described above, a slow increase in internal FITC-IgE is observed in the absence of crosslinking. Furthermore, the percentage of cell-associated FITC-IgE internalized after 8 hours in this pulse-chase experiment (approx. 30%) is only slightly less than that observed after continuous overnight incubation with excess FITC-IgE, as described above. As expected, the rate of internalization of FITC-IgE in the presence of anti-IgE is much greater than in the absence of crosslinking, and internalization in the presence of anti-IgE is near the maximal value of 80% at the earliest time point examined (approx. 2 hours after anti-IgE addition). Because FITC fluorescence in early and
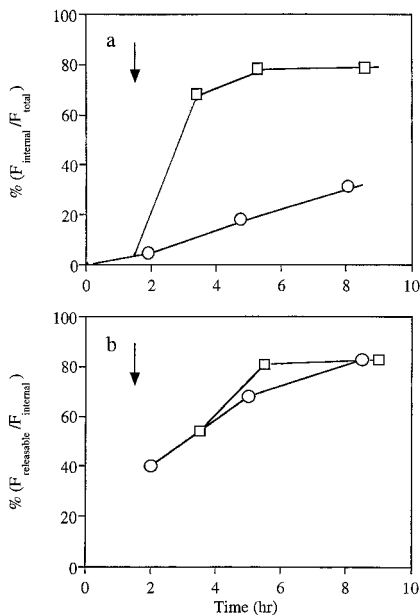
Fig. 7. Pulse-chase experiment showing the time course of FITC-IgE quenching due to internalization (a) and the percentage of internal FITC-IgE that is released upon cell activation (b). □, cells labeled for 1 hour with FITC-IgE and treated with 1.6 mg/ml anti-IgE (added at the arrow); ○, labeled, untreated cells. The parameters shown were calculated from equations 1 and 2.

perinuclear endosomes is not completely quenched (Fig. 5i), internalization measured by FITC fluorescence quenching (equation 2) provides a lower limit to the amount of internal FITC-IgE. Control experiments showed that binding and crosslinking by anti-IgE under conditions that do not permit internalization (lower temperatures or in the presence of cytochalasin D at 37°C) do not cause significant FITC quenching (data not shown). Both in the presence and in the absence of anti-IgE, the total amount of cell-associated FITC (determined after Triton X-100 addition) remained constant during the entire 9 hour incubation period (data not shown), indicating little or no loss of internalized, degraded IgE.

Fig. 7b shows the time course of delivery of internalized FITC-IgE to secretory vesicles that undergo exocytosis in response to optimal stimulation. For cells in the absence of anti-IgE (○), the fraction of internal FITC-IgE that is released after stimulation (equations 1, 2) with A23187 and PMA in the presence of cytochalasin D continues to increase throughout the 8.5 hour time period following the initiation of FITC-IgE binding, indicating that delivery of internalized FITC-IgE to secretory vesicles is a relatively slow process that is not entirely limited by the rate of internalization. This conclusion is substantiated by the results in Fig. 7b for cells treated with anti-IgE (□), which do not reach a maximal value for the percentage of internal FITC-IgE that is releasable by stimulation until approx. 4 hours after the addition of crosslinking ligand. Because most of the FITC-IgE-FcεRI internalized in response to anti-IgE is delivered initially to perinuclear endosomes (Fig. 5i; Robertson et al., 1986), it appears that labeling of secretory vesicles by crosslinked FITC-IgE occurs after transit through this organelle. The slightly slower rate of appearance of internalized monomeric

FITC-IgE in secretory vesicles compared with that for FITC-IgE crosslinked by anti-IgE suggests that monomeric FITC-IgE also passes through a similar rate-limiting endosomal compartment.

A surprising aspect of these findings for both cases is that, although slow, the delivery of internalized FITC-IgE label to secretory vesicles is a very efficient (i.e. high yield) process. For cells treated with anti-IgE, approx. 80% of the internalized FITC-IgE is releasable upon stimulation after 4 hours of treatment. At this time, approx. 80% of the cell-bound FITC-IgE is internal, so that >60% of the FITC-IgE initially bound to FcεRI at the cell surface is delivered to the secretory vesicles (Fig. 7a,b). For cells with monomeric IgE bound to FcεRI, the percentage of internalized FITC-IgE that is releasable reaches approx. 80% by 8.5 hours after binding is initiated (Fig. 7b). At this time, less than 40% has internalized (Fig. 7a), so that the percentage of FITC-IgE initially bound that is delivered to secretory granules is approx. 30%. Implications of these results for the relationship of secretory granules and endosomal trafficking in these cells are discussed below.

Exocytosis visualized by confocal microscopy after labeling granules with Cy3-IgE

To investigate FcεRI-mediated degranulation in individual live cells, we labeled their secretory vesicles with Cy3-IgE. Cells incubated overnight with Cy3-IgE exhibit brightly labeled peripheral vesicles, as well as some dimmer surface label corresponding to monomeric Cy3-IgE bound to FcεRI (Fig. 8b). Fig. 8d shows that stimulation with an optimal dose of DNP-BSA for 45 minutes at 37°C prior to confocal imaging results in cells that retain their surface label but have substantially less intracellular label. Stimulation with Ca^{2+} ionophore and PMA causes larger loss of intracellular Cy3 label (Fig. 8f), and this correlates with the generally more efficient stimulation of degranulation by these reagents than by DNP-BSA in suspended cells (our unpublished observations). To quantify this experiment, individual bright internal spots were counted in equatorial images of 15-30 cells before and after stimulation. Approximately 60-70% of these spots disappeared 45 minutes after stimulation with DNP-BSA; approximately 80% disappeared 30 minutes after stimulation with A23187 and PMA.

Colocalization of Cy3-labeled granules to serotonin-labeled granules

To identify the low pH peripheral vesicles that accumulate degraded FITC-IgE and Cy3-IgE, we compared the distribution of internal Cy3 label to that of serotonin-labeled secretory granules. Maiti et al. (1997) recently demonstrated that exogenous serotonin taken up into RBL-2H3 mast cell granules can be imaged using three-photon excitation. Fig. 9a shows such an image for RBL-2H3 cells that have been labeled overnight by incubation with 0.10 mM serotonin together with a small excess of Cy3-IgE over receptors. The brighter, punctate fluorescence seen in most cells in this image is only detected following loading with exogenous serotonin, indicating that it is serotonin taken up into secretory granules (Maiti et al., 1997 and data not shown). The dimmer fluorescence seen to be more uniformly distributed throughout the cells in Fig. 9a and also seen as green intracellular 'background' in Fig. 9c is observed in the absence of serotonin

Fig. 8. Differential interference contrast (a,c,e) and confocal fluorescence (b,d,f) images of Cy3-IgE-labeled cells reveal degranulation of individual cells. RBL-2H3 cells were sensitized overnight with excess Cy3-anti-DNP-IgE. (a,b) Suspended cells before addition of triggering reagents. (c,d) Cells triggered with 20 ng/ml DNP-BSA for 45 minutes at 37°C before imaging. (e,f) Cells triggered with 50 nM PMA plus 200 nM A23187 for 30 minutes at 37°C before imaging. Bar, 10 μm.
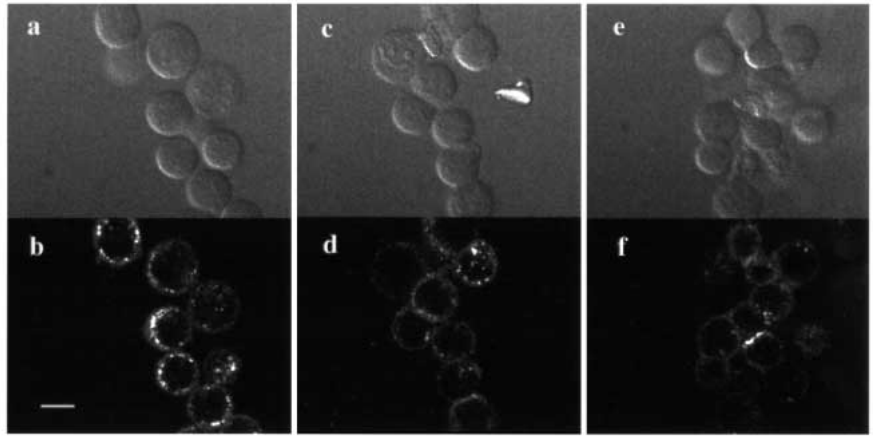
loading and is due mostly to tryptophan fluorescence from cellular proteins. Stimulation of RBL-2H3 cells with antigen results in the loss of the punctate serotonin emission from the labeled granules (R. M. Williams, J. B. Shear, W. R. Zipfel, S. Maiti and W. W. Webb, unpublished observations).

Fig. 9b shows Cy3-IgE fluorescence in the same cells excited using a two-photon process with the same illumination beam. Bright punctate fluorescence is seen to be co-localized with that of the punctate serotonin fluorescence in Fig. 9a. Fig. 9c shows a two-color overlay of the serotonin image (green) and the Cy3-IgE image (red). Colocalization of most punctate Cy3-IgE with punctate serotonin label is indicated by the propensity for yellow-to-orange spots compared with occasional red spots for Cy3-IgE alone (e.g. see Fig. 9c, bottom middle cell). Colocalization analysis of 39 pairs of images shows that 65±12% of the punctate fluorescence in Cy3 images

is colocalized to that in the serotonin images. Coincidental colocalization, as determined by the same analysis of randomized image pairs, is 5±3%.

Further evidence for co-localization of these labels in the same intracellular vesicles comes from steady-state fluorescence measurements of cells labeled with serotonin and Cy3-IgE. In these experiments, we found that the Cy3-IgE label is quenched by an average of 41±4% in five different samples by the exogenous serotonin taken up by the cells (data not shown). This quenching is most likely due to direct interactions between Cy3 and serotonin, providing further support for their co-localization in the same organelles. From these results, it is likely that vesicles containing the highest concentrations of serotonin will exhibit less Cy3 fluorescence than others with lower amounts of serotonin, and this may contribute to the variable yellow and orange colors seen in
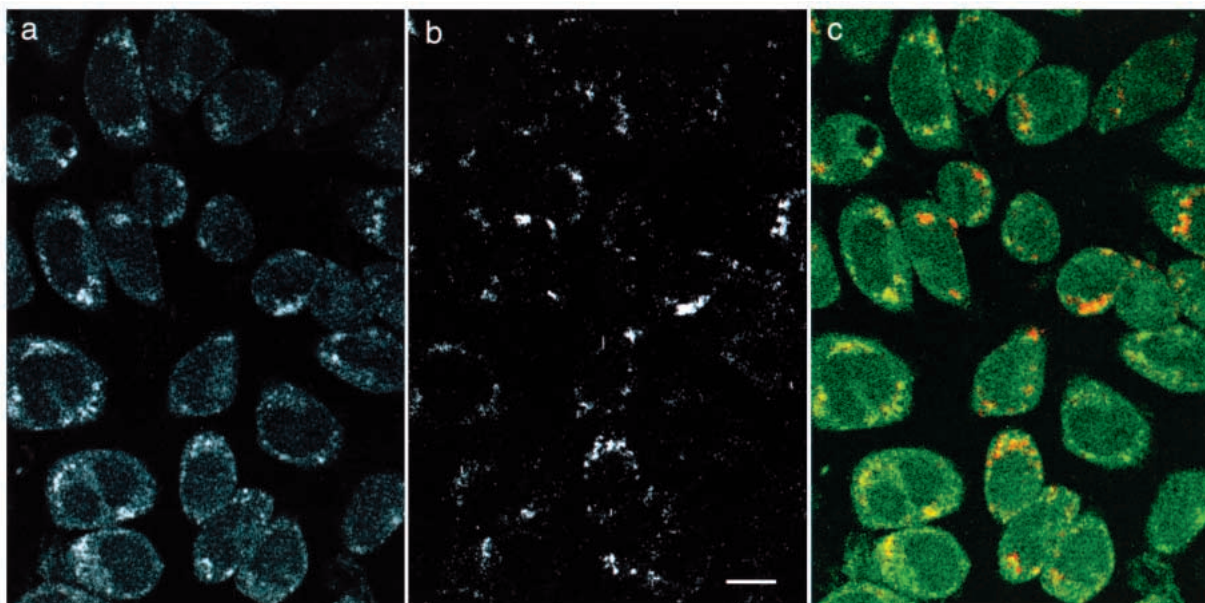

Fig. 9. Comparison of the distribution of serotonin-labeled granules (a) and internalized Cy3-IgE (b) using multi-photon imaging of live RBL-2H3 cells. Following overnight incubation with 0.10 mM serotonin and 1.5 μg/ml Cy3-IgE, attached cells were washed with BSS and images were collected. In the two-color overlay image (c), green represents emission resulting from the serotonin excitation wavelength and red represents that from the Cy3 excitation wavelength. Labeled granules containing both serotonin and Cy3 have yellow-to-orange tints. The more uniform intracellular green fluorescence is due to non-serotonin emission. Bar, 10 μm.

different cells in Fig. 9c. Thus, the co-localization detected in Fig. 9 represents a lower limit to the actual co-localization of serotonin with intracellular Cy3 label.

DISCUSSION

This study shows that incubating RBL-2H3 cells overnight with fluorescently labeled monomeric IgE results in slow endocytosis of this FcεRI-bound IgE and efficient accumulation of internalized fluorescent IgE fragments in highly acidic intracellular vesicles. Most of this label is released in response to stimuli that trigger degranulation in these cells, including ligands that cause aggregation of FcεRI, and the kinetics of this release are identical to those of an established granule marker, β-hexosaminidase. These results suggest that a large fraction of the fluorescently labeled vesicles are true secretory granules. Consistent with this, simultaneous multiphoton serotonin and Cy3-IgE images show that a large fraction of the vesicles labeled with fluorescent IgE under these conditions also contain the secretory granule marker serotonin (Fig. 9). Thus, IgE bound to FcεRI is endocytosed, degraded and preferentially delivered to secretory granules, from which it is released in response to aggregation of FcεRI at the cell surface.

It is remarkable that fluorescent IgE bound to FcεRI at the cell surface is delivered to these secretory vesicles so efficiently: for both monomeric FITC-IgE and FITC-IgE internalized by aggregation with anti-IgE, approx. 80% of the internalized label is delivered to the secretory granules after 5-8 hours (Fig. 7b). In the pulse-chase experiments, the fraction of FITC-IgE initially bound to FcεRI that is delivered to secretory vesicles is approx. 0.6 for cells treated with anti-IgE and approx. 0.3 for cells without anti-IgE treatment. There was no significant loss of fluorescence from the cells during the 9-hour time period. During a similar time period, FITC-cholera toxin subunit B bound to ganglioside GM1 on these cells is internalized but does not preferentially accumulate in the secretory vesicles labeled by fluorescent IgE (D. Holowka, unpublished results). This indicates that the delivery of fluorescent IgE to secretory vesicles is not simply the entrapment of degraded fluorescent peptides in these vesicles, but results from a more selective trafficking process.

Despite this highly efficient delivery of internalized FITC-IgE to regulated secretory vesicles, the process is slow, even for the cells in which the internalization of FITC-IgE is accelerated by aggregation with anti-IgE. In this latter case, the $t_{1/2}$ for delivery of internalized FITC-IgE to secretory granules is approx. 2 hours, and maximal accumulation occurs approx. 4 hours after endocytosis is initiated by anti-IgE (Fig. 7b). As the appearance of FITC label in perinuclear endosomes is detectable within minutes after addition of excess anti-IgE (Fig. 5i), the rate-limiting step for appearance in peripheral secretory vesicles must be subsequent to these events.

The mechanism by which internalized fluorescent IgE is delivered to the secretory granules is not yet known. The turnover of cell surface IgE receptors is slow ($t_{1/2}$ = 8-24 hours; Furuichi et al., 1985; Quarto et al., 1985) compared with bulk plasma membrane endocytosis ($t_{1/2} \simeq 1$ hour; Mayor et al., 1993), and no evidence for FcεRI recycling has been found (Isersky et al., 1979). These observations suggest the existence

of interactions of FcεRI at the plasma membrane, which hinder its internalization prior to aggregation. Aggregated, internalized IgE-FcεRI traffics to perinuclear endosomes prior to delivery of IgE to more peripheral secretory vesicles, and it is likely that monomeric IgE-FcεRI follows a similar route, since the time course of this process is similarly slow for both conditions (Fig. 7b). The pH of early and perinuclear endosomes is greater than 5.5 (Mukherjee et al., 1997), and this is not sufficiently acidic to promote dissociation of IgE from FcεRI, which requires pH<4.5 for detectable dissociation (Kulczycki and Metzger, 1974). Because of this, it is unlikely that dissociated IgE is delivered to late endosomes and lysosomes as a component of bulk luminal fluid. It is possible that FcεRI contains a targeting sequence (Trowbridge et al., 1993), which causes retention of internalized IgE-receptor complexes in the perinuclear endosome, sometimes referred to as the 'recycling endosome' (Mukherjee et al., 1997), thus preventing default recycling and facilitating transport to lysosomes/secretory granules. Alternatively, retention of monomeric IgE-receptor complexes in a sorting endosome by some physical segregation, such as lateral phase separation (Mukherjee et al., 1997), might lead to eventual delivery to late endosomes, where proteolytic degradation of IgE could result in accumulation of labeled IgE fragments in the lumen of the secretory granules.

Our results indicate that regulated secretory lysosomes represent a major population of the secretory organelles in the RBL cells. The low pH of these secretory organelles, together with the stimulated release of >80% of the lysosomal marker, β-hexosaminidase (Fig. 4), suggest that most lysosomes act as regulated secretory vesicles in these cells. As shown here, the kinetics and dose-dependence of antigen-stimulated release of β-hexosaminidase and FITC-IgE fragments are identical (Figs 3 and 4), and other experiments showed that the percentage of endogenous β-hexosaminidase and exogenously added ³H-serotonin released by an optimal dose of antigen are very similar (K. Subramanian, N. T. Harris, D. Holowka and B. Baird, unpublished results). Although we cannot exclude the presence of a subset of granules with a non-lysosomal character, the majority of secretory granules in these cells have the properties of lysosomes, and this appears to account for the unusual trafficking patterns for internalized IgE-FcεRI that we observe.

The lysosomal characteristics of secretory granules in RBL-2H3 cells are reminiscent of the lytic granules in natural killer cells and cytotoxic T lymphocytes, which kill their target cells by regulated exocytosis of both lysosomal and secretory components from these granules (Griffiths and Aragon, 1995). In support of this relationship, Henkart and colleagues showed that transfection of RBL-2H3 cells with perforin and granzyme A allows these cells to effect specific IgE-FcεRI-mediated killing of nucleated target cells (Shriver et al., 1992). The abundance of acid hydrolases in normal mast cell granules (Schwartz and Austen, 1984) is also consistent with lysosomal characteristics for secretory vesicles in these cells. We recently found that the regulated exocytic vesicles in RBL-2H3 cells can also be labeled by FITC-dextran in a process that requires micromolar concentrations for a similar amount of labeling to that achieved by nanomolar concentrations of FITC-IgE. This low-level internalization of FITC-dextran presumably occurs in a non-specific manner via fluid-phase pinocytosis (Pfeiffer

et al., 1985). Once internalized, the efficiency of delivery of FITC-dextran to secretory vesicles is similar to that for internalized FITC-IgE, but the rate of dextran delivery to these vesicles is somewhat faster, suggesting that it may occur through a different trafficking route (K. Xu, D. Holowka and B. Baird, unpublished observations). Earlier studies on mouse mast cells and guinea pig basophils provided electron microscopic evidence for delivery of extracellular peroxidase to cytoplasmic granules by endocytosis (Dvorak et al., 1985). Taken together, these various results suggest that most secretory granules in RBL-2H3 mast cells, and possibly in other mast cells, have characteristics common to lysosomes, serving as the terminus of the degradative endocytic pathway.

Our results are somewhat different from those of Isersky et al. (1979), who concluded that there was no significant time-dependent internalization of monomeric IgE during extended incubations with ^{125}I-IgE at 37°C. Their study used acidic dissociation of peripheral ^{125}I-IgE and ^{125}I-IgE autoradiography to detect internalized IgE-FcεRI, and it is possible that a small amount of peripherally located internal ^{125}I-IgE would not be detected, as the spatial resolution of the latter method is limited (Isersky et al., 1979). It is unlikely that our results are dependent on the specific labels used, since the same localization to regulated secretory vesicles occurs for IgE modified with two fluorescent probes that are chemically very different from each other. We have recently observed that the extent and kinetics of antigen-stimulated IgE-FcεRI internalization for RBL-2H3 cells can vary significantly depending on culture conditions (D. Holowka, unpublished results). Such differences might also affect the rate of endocytosis and delivery to secretory granules of monomeric IgE-FcεRI.

Our confocal microscopy results with Cy3-IgE, which efficiently labels the secretory vesicles releasable by FcεRI-mediated stimulation, indicate that this approach should allow real-time analysis of receptor-mediated exocytosis in individual cells. At least some of these labeled vesicles are large enough to permit their tracking during conditions of stimulation, such that spatial and temporal redistribution of individual vesicles and loss of fluorescence from these vesicles should be observable. The molecular mechanism for the terminal steps of FcεRI-mediated exocytosis is largely unknown for RBL-2H3 cells as well as for peritoneal mast cells. Thus, a simple method for fluorescent labeling of exocytic vesicles should be valuable for identification of individual degranulating cells and for monitoring the dynamics of the exocytic process in individual cells, as well as for detailed analysis of the kinetics of the exocytosis under conditions in which critical components of this process are genetically altered (Geppert et al., 1994).

In conclusion, our studies reveal efficient delivery of endocytosed FcεRI-bound IgE to regulated secretory granules, indicating that these granules serve as terminal degradative organelles in RBL-2H3 mast cells, a function normally assigned to lysosomes in most cell types. Furthermore, the stimulated release of fluorescent IgE fragments that we observe provides a simple fluorescence method for monitoring the kinetics of stimulated exocytosis. Confocal microscopy analyses with Cy3-IgE demonstrate that the fluorescence method we have developed for labeling secretory granules should be useful for single-cell measurements of receptor-mediated exocytosis. It is also possible to use this method in combination with other fluorescent probes, such as indicators of cytoplasmic Ca^{2+}, to investigate spatial and temporal relationships between these different processes monitored simultaneously. These approaches should allow important questions regarding the mechanism of receptor-mediated exocytosis to be directly addressed in future studies.

REFERENCES

Alber, G., Kent, U. M. and Metzger, H. (1992). Functional comparison of FcεRI, FcγRII and FcγRIII in mast cells. *J. Immunol.* **149**, 2428-2436.

Barsumian, E. L., Isersky, C., Petrino, M. G. and Siraganian, R. P. (1981). IgE-induced histamine release from rat basophilic leukemia cell lines: isolation of releasing and nonreleasing clones. *Eur. J. Immunol.* **11**, 317-323.

Bonifacino, J. S., Perez, P., Klausner, R. D. and Sandoval, I. V. (1986). Study of the transit of an integral membrane protein from secretory granules through the plasma membrane of secreting rat basophilic leukemia cells using a specific monoclonal antibody. *J. Cell Biol.* **102**, 516-522.

Bonifacino, J. S., Yuan, L. and Sandoval, I. V. (1989). Internalization and recycling to serotonin-containing granules of the 80K integral membrane protein exposed on the surface of secreting rat basophilic leukemia cells. *J. Cell Sci.* **92**, 701-712.

Chang, E.-Y., Zheng, Y., Holowka, D. and Baird, B. (1995). Alteration of lipid composition modulates FcεRI signaling in RBL-2H3 cells. *Biochemistry* **34**, 4376-4384.

Cunha-Melo, J. R., Gonzaga, H. M., Ali, H., Huang, F. L., Huang, K. P. and Beaven, M. A. (1989). Studies of protein kinase C in the rat basophilic leukemia (RBL-2H3) cell reveal that antigen-induced signals are not mimicked by the actions of phorbol myristate acetate and Ca^{2+} ionophore. *J. Immunol.* **143**, 2617-2625.

Dangl, J. L., Wensel, T. G., Morrison, S. L., Stryer, L., Herzenberg, L. A. and Oi, V. T. (1988). Segmental flexibility and complement fixation of genetically engineered chimeric human, rabbit and mouse antibodies. *EMBO J.* **7**, 1989-1994.

Dvorak, A., Klebanoff, S. J., Henderson, W. R., Monahan, R. A., Pyne, K. and Galli, S. J. (1985). Vesicular uptake of eosinophil peroxidase by guinea pig basophils and by cloned mouse mast cells and granule-containing lymphoid cells. *Am. J. Pathol.* **118**, 425-438.

Erickson, J., Kane, P., Goldstein, B., Holowka, D. and Baird, B. (1986). Cross-linking of IgE-receptor complexes at the cell surface a fluorescence method for studying the binding of monovalent and bivalent haptens to IgE. *Mol. Immunol.* **23**, 769-782.

Field, K. A., Holowka, D. and Baird, B. (1997). Compartmentalized activation of the high affinity immunoglobulin E receptor within membrane domains. *J. Biol. Chem.* **272**, 4276-4280.

Furuichi, K., Rivera, J. and Isersky, C. (1984). The fate of IgE bound to rat basophilic leukemia cells III: Relationship between antigen-induced endocytosis and serotonin release. *J. Immunol.* **133**, 1513-1520.

Furuichi, K., Rivera, J. and Isersky, C. (1985). The receptor for immunoglobulin E on rat basophilic leukemia cells: effect of ligand binding on receptor expression. *Proc. Nat. Acad. Sci. USA* **82**, 1522-1525.

Galli, S. J., Dvorak, A. M. and Dvorak, H. F. (1984). Basophils and mast cells: morphologic insights into their biology, secretory patterns, and function. *Prog. Allergy* **34**, 1-141.

Geppert, M., Goda, Y., Hammer, R. E., Li, C., Rosanl, T. W., Stevens, C. F. and Sudhof, T. C. (1994). Synaptotagmin I: a major Ca^{2+} sensor for transmitter release at a central synapse. *Cell* **79**, 717-727.

Gomperts, B. D. (1990). G$_E$: a GTP-binding protein mediating exocytosis. *Ann. Rev. Physiol.* **52**, 591-606.

Griffiths, G. M. and Argon, Y. (1995). Structure and biogenesis of lytic granules. *Curr. Top. Microbiol. Immunol.* **198**, 39-58.

Griffiths, G. M. (1996). Secretory lysosomes - a special mechanism of regulated secretion in haemopoietic cells. *Trends Cell Biol.* **6**, 329-332.

Holowka, D. and Baird, B. (1996). Antigen-mediated IgE receptor aggregation and signaling: A window on cell surface structure and dynamics. *Ann. Rev. Biophys. Biomol. Struct.* **25**, 79-112.

Holowka, D. and Metzger, H. (1982). Further characterization of the β-component of the receptor for immunoglobulin E. *Mol. Immunol.* **19**, 219-227.

Isersky, C., Rivera, J., Mims, S. and Triche, T. J. (1979). The fate of IgE bound to rat basophilic leukemia cells. *J. Immunol.* **122**, 1926-1936.

Isersky, C., Rivera, J., Segal, D. M. and Triche, T. (1983). The fate of IgE bound to rat basophilic leukemia cells II: Endocytosis of IgE oligomers and effect on receptor turnover. *J. Immunol.* **131**, 388-396.

Kulczycki, A., Jr. and Metzger, H. (1974). The interaction of IgE with rat basophilic leukemia cells II: Quantitative aspects of the binding reaction. *J. Exp. Med.* **140**, 1676-1695.

Liu, F., Bohn, J. W., Ferry, E. L., Yamamoto, H., Molinaro, C. A., Sherman, L. A., Klinman, N. R. and Katz, D. (1980). Monoclonal dinitrophenol specific murine IgE antibody: purification, isolation, and characterization. *J. Immunol.* **124**, 2728-2736.

Maiti, S., Shear, J. B., Williams, R. M., Zipfel, W. R. and Webb, W. W. (1997). Measuring serotonin distribution in live cells with three-photon excitation. *Science* **275**, 530-532,

Mao, S. Y., Pfeiffer, J. R., Oliver, J. M. and Metzger, H. (1993). Effects of subunit mutation on the localization to coated pits and internalization of cross-linked IgE-receptor complexes. *J. Immunol.* **151**, 2760-2774.

Mayor, S., Presley, J. F. and Maxfield, F. R. (1993). Sorting of membrane components from endosomes and subsequent recycling to the cell surface occurs by a bulk flow process. *J. Cell Biol.* **121**, 1257-1268.

Mohr, F. C. and Fewtrell, C. (1987). Depolarization of rat basophilic leukemia cells inhibits calcium uptake and exocytosis. *J. Cell Biol.* **104**, 783-792.

Mukherjee, S., Ghosh, R. and Maxfield, F. R. (1997). Endocytosis. *Physiol. Reviews* **77**, 759-803.

Narasimhan, V., Holowka, D. and Baird, B. (1990). Microfilaments regulate the rate of exocytosis in rat basophilic leukemia cells. *Biochem. Biophys. Res. Commun.* **171**, 222-229.

Ohkuma, S. and Poole, B. (1978). Fluorescence probe measurement of the intralysosomal pH in living cells and the perturbation of pH by various agents. *Proc. Nat. Acad. Sci. USA* **75**, 3327-3331.

Ortega, E. and Pecht, I. (1988). A monoclonal antibody that inhibits secretion from rat basophilic leukemia cells and binds to a novel membrane component. *J. Immunol.* **141**, 4324-4332.

Pfeiffer, J. R., Seagrave, J. C., Davis, B. H., Deanin, G. G. and Oliver, J. M. (1985). Membrane and cytoskeletal changes associated with IgE-mediated serotonin release from rat basophilic leukemia cells. *J. Cell Biol.* **101**, 2145-2155.

Pierini, L., Holowka, D. and Baird, B. (1996). FcεRI-mediated association of 6-um beads with RBL-2H3 mast cells results in exclusion of signaling proteins from the forming phagosome and abrogation of normal downstream signaling. *J. Cell Biol.* **134**, 1427-1439.

Quarto, R., Kinet, J.-P. and Metzger, H. (1985). Coordinate synthesis and degradation of the α-, β- and γ-subunits of the receptor for immunoglobulin E. *Molec. Immunol.* **22**, 1045-1051.

Ra, C., Furuichi, K., Rivera, J., Mullins, J. M., Isersky, C. and White, K. N. (1989). Internalization of IgE receptors on rat basophilic leukemic cells by phorbol ester comparison with endocytosis induced by receptor aggregation. *Eur. J. Immunol.* **19**, 1771-1778.

Robertson, D., Holowka, D. and Baird, B. (1986). Cross-linking of IgE-receptor complexes induces their interaction with the cytoskeleton of rat basophilic leukemia cells. *J. Immunol.* **136**, 4565-4572.

Schwartz, L. B., Lewis, R. A., Seldin, D. and Austen, K. F. (1981). Acid hydrolases and tryptase from secretory granules of dispersed human lung mast cells. *J. Immunol.* **126**, 1290-1294.

Schwartz, L. B. and Austen, K. F. (1984). Structure and function of the chemical mediators of mast cells. *Prog. Allergy* **34**, 271-321.

Seagrave, J. and Oliver, J. M. (1990). Antigen-dependent transition of IgE to a detergent-insoluble form is associated with reduced IgE receptor-dependent secretion from RBL- 2H3 mast cells. *J. Cell Physiol.* **144**, 128-136.

Seldin, D. C., Adelman, S., Austen, K. F., Stevens, R. L., Hein, A., Caulifield, J. P. and Woodburg, R. G. (1985). Homology of the rat basophilic leukemia cell and the rat mucosal mast cell. *Proc. Nat. Acad. Sci. USA* **82**, 3871-3875.

Shriver, J. W., Su, L. and Henkart, P. A. (1992). Cytotoxicity with target DNA breakdown by rat basophilic leukemia cells expressing both cytolysin and granzyme A. *Cell* **71**, 315-322.

Subramanian, K., Holowka, D., Baird, B. and Goldstein, B. (1996). The Fc segment of IgE influences the kinetics of dissociation of a symmetrical bivalent ligand from cyclic dimeric complexes. *Biochemistry* **35**, 5518-5527.

Taurog, J. D., Fewtrell, C. and Becker, E. L. (1979). IgE mediated triggering of rat basophil leukemia cells: lack of evidence for serine esterase activation. *J. Immunol.* **122**, 2150-2153.

Trowbridge, I. S., Collawn, J. F. and Hopkins, C. R. (1993). Signal-dependent membrane protein trafficking in the endocytic pathway. *Annu. Rev. Cell Biol.* **9**, 129-161.

Weetall, M., Shopes, B., Holowka, D., and Baird, B. (1990). Mapping the site of interaction between murine IgE and its high affinity receptor with chimeric Ig. *J. Immunol.* **145**, 3849-3854.

Weetall, M., Holowka, D. and Baird, B. (1993). Heterologous desensitization of the high affinity receptor for IgE, FcεRI, on RBL cells. *J. Immunol.* **150**, 4072-4083.

White, K. N. and Metzger, H. (1988). Translocation of protein kinase C in rat basophilic leukemic cells induced by phorbol ester or by aggregation of IgE receptors. *J. Immunol.* **141**, 942-947.

WoldeMussie, E., Maeyama, K. and Beaven, M. A. (1986). Loss of secretory response of rat basophilic leukemia (2H3) cells at 40°C is associated with reversible suppression of inositol phospholipid breakdown and calcium signals. *J. Immunol.* **137**, 1674-1680.

Xu, K., Goldstein, B., Holowka, D. and Baird, B. (1998). Kinetics of multivalent antigen DNP-BSA binding to IgE-FcεRI in relationship to the stimulated tyrosine phosphorylation of FcεRI. *J. Immunol.* **160**, 3225-3235.